Accepted Manuscript

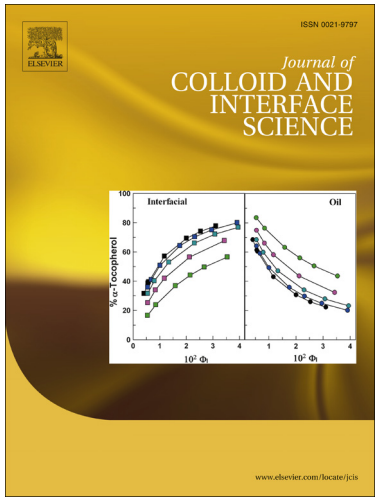

Short Communication

Bias-dependent effects in planar perovskite solar cells based on $CH_3NH_3PbI_{3-x}Cl_x$ films

Miaoqiang Lyu, Jung-Ho Yun, Rasin Ahmed, Daniel Elkington, Qiong Wang, Meng Zhang, Hongxia Wang, Paul Dastoor, Lianzhou Wang

PII: S0021-9797(15)00418-X
DOI: http://dx.doi.org/10.1016/j.jcis.2015.04.041
Reference: YJCIS 20421

To appear in: *Journal of Colloid and Interface Science*

Received Date: 20 March 2015
Accepted Date: 18 April 2015

Please cite this article as: M. Lyu, J-H. Yun, R. Ahmed, D. Elkington, Q. Wang, M. Zhang, H. Wang, P. Dastoor, L. Wang, Bias-dependent effects in planar perovskite solar cells based on $CH_3NH_3PbI_{3-x}Cl_x$ films, *Journal of Colloid and Interface Science* (2015), doi: http://dx.doi.org/10.1016/j.jcis.2015.04.041

Bias-dependent effects in planar perovskite solar cells based on $CH_3NH_3PbI_{3-x}Cl_x$ films

Miaoqiang Lyu [a], Jung-Ho Yun [a], Rasin Ahmed [b], Daniel Elkington [c], Qiong Wang [a], Meng Zhang [a], Hongxia Wang [b*], Paul Dastoor [c*], Lianzhou Wang [a*]

[a] *Nanomaterials Centre, School of Chemical Engineering and AIBN, the University of Queensland, St Lucia, Brisbane, QLD 4072, Australia.*

Email: l.wang@uq.edu.au,

[b] *School of Chemistry, Physics and Mechanical Engineering, Science and Engineering Faculty, Queensland University of Technology, Brisbane, QLD 4001, Australia..*

Email: hx.wang@qut.edu.au;

[c] *Centre for Organic Electronics, University of Newcastle, University Drive, Callaghan NSW 2308, Australia.*

Email: Paul.Dastoor@newcastle.edu.au

Abstract

A unique bias-dependent phenomenon in $CH_3NH_3PbI_{3-x}Cl_x$ based planar perovskite solar cells has been demonstrated, in which the photovoltaic parameters derived from the current-voltage (I-V) curves are highly dependent on the initial positive bias of the I-V measurement. In FTO/$CH_3NH_3PbI_{3-x}Cl_x$/Au devices, the open-circuit voltage and short-circuit current increased by *ca*. 337.5% and 281.9% respectively, by simply increasing the initial bias from 0.5 V to 2.5 V.

Keywords: perovskite solar cells; bias-dependent effect; $CH_3NH_3PbI_{3-x}Cl_x$; current-voltage hysteresis; current-voltage measurement

Introduction

Organic-inorganic hybrid perovskite solar cells (PSCs) have attracted much recent research attention as one of the most promising photovoltaic technologies, capable of delivering high efficiencies of over 16%.[1-3] To date, the commonly adopted perovskite materials for PSCs are methylammonium lead iodide ($CH_3NH_3PbI_3$) and its mixed halide counterparts. Although $CH_3NH_3PbI_{3-x}Cl_x$ perovskite shows a similar band-gap and crystal structure compared with $CH_3NH_3PbI_3$, it shows several unique properties such as a much longer electron diffusion length (up to ~1 μm) and a giant dielectric constant enhanced by light illumination or external electrical bias.[4, 5] Moreover, the $CH_3NH_3PbI_{3-x}Cl_x$ film shows abnormal charge accumulation, slow dynamic processes within the perovskite film and current-voltage (I-V) hysteresis.[6-9] The anomalous hysteresis in the I-V measurement has been a focus of studies and much work has been performed in order to explore measurement parameters that may affect the hysteresis, such as I-V scan rate, scan directions, delay time, light illumination and different device structures. [8-13] Snaith *et al.* suggested that a contact resistance between the perovskite and TiO_2 could be the key reason for the hysteresis, while they also discussed possible influence of polarization in the perovskite films. [8] However, current hysteresis studies have been mostly based on complete perovskite devices with electron/hole selective layers. Perovskite devices without these selective layers may provide more convincing evidence on the origin of the hysteresis issue, yet rare works have been published in this area. Recently, Wei *et al.* observed that different scanning biases can affect the current-voltage curves of $CH_3NH_3PbI_3$-based perovskite solar cells and increasing positive biases can enhance the photocurrent density to some extent.[14] More recently, Chen *et al.* investigated the electric poling effect on performance of $CH_3NH_3PbI_3$-based perovskite solar cells, in which they found that negative electric poling could decrease the device performance by

probably reducing the built-in electric field, while on the other hand, positive electric poling may improve the device performance.[15, 16] However, there is still limited systematic study on whether or how the $CH_3NH_3PbI_{3-x}Cl_x$-based perovskite films in an assembled PSC device respond to the external bias applied during the I-V measurements, especially based on a capacitor-like device. Also, there is little direct experimental evidence on the origin of the I-V hysteresis.

Herein, we demonstrate a systematic study on an interesting bias-dependent effect of the $CH_3NH_3PbI_{3-x}Cl_x$-based PSCs, whereby different initial electrical biases during the reverse I-V scan (from positive bias to 0 V) have a significant effect on the device parameters. Furthermore, we provide direct evidence to confirm that both the bias-dependent effect and I-V hysteresis phenomenon are resulted from the $CH_3NH_3PbI_{3-x}Cl_x$ layer itself, which has not been reported previously. The new phenomenon reported here can be of importance to set standardised testing method and to design better PSCs.

Experimental section

Preparation of perovskite:

Typically, 24 ml of methylamine (33wt% in absolute ethanol), 10 ml of hydroiodic acid (55wt% in water), and 100 ml of absolute ethanol were mixed at 0℃ to react for 2 h and MAI was crystallized by a rotary evaporator at 50℃. A yellowish powder was obtained, which turned to white colour after re-crystallization in the absolute ethanol and diethyl ether. Finally, the powder was dried in a vacuum oven at 60 ℃ for 12 h.

Chlorine-doped perovskite solution ($CH_3NH_3PbI_{3-x}Cl_x$) was prepared by mixing MAI and lead (II) chloride at a 3:1 in molar ratio with a concentration of 50wt% in anhydrous N, N-Dimethylformamide (DMF) solution. Tri-iodide perovskite ($CH_3NH_3PbI_3$) solution was

prepared by mixing MAI and lead (II) chloride at a 1:1 in molar ratio with a concentration of 40wt% in anhydrous DMF solution. The solution was filtered by 0.45 μm syringe filter before use.

Solar cell assembly:

Fluorine-doped tin oxide (FTO) coated glass substrates (FTO22-7, Yingkou OPV Tech New Energy Co. Ltd) were etched with 2 M HCl aqueous solution and Zinc powder. Then the substrates were cleaned subsequently in acetone, ethanol and isopropanol, and dried under nitrogen gas flow. Prior to the spray pyrolysis deposition of TiO_2 compact layer, the substrates were cleaned by oxygen plasma (RIE, ATX-600, 30W) for 10 min. The spray pyrolysis deposited TiO_2 blocking layers were post-treated with 0.2 M $TiCl_4$ aqueous solution at 70 ℃ for 0.5 h, followed by annealing at 500 ℃ for 30 min. The perovskite solution was dispensed onto the $TiCl_4$-treated substrates and spin-coated at 2500 revolutions per minute (RPM) for 30 s in air with 2500 RPM/s ramping rate. After annealing treatment at 100 ℃ for 45 min on a hotplate in the air, the substrates were left cooling down and spin-coated with P3HT (MW 54000-75000, Sigma-Aldrich, 15mg/ml in 1, 2-dichlorobenzene) at 2000 RPM for 30s. The coated substrates were further annealed at 100 ℃ for 15 min to remove the remaining solvent and left in the dark in the glove box overnight before the gold deposition of 60 nm by e-beam evaporation (Temescal FC-2000). The cell area was defined by a metal mask with an aperture area of 0.07 cm^2.

For the assembly of the device P1 (FTO/ $CH_3NH_3PbI_{3-x}Cl_x$ /Au), a different spin-coating condition was used to deposit thicker perovskite film in order to avoid short-circuit of the device due to direct contact between the gold layer and the FTO substrate. In brief, the perovskite solution was dispensed onto the FTO substrate and spin-coated at 1000 RPM for 30 s in air with a 200 RPM/s ramping rate, followed by annealing at 100 ℃ for 120 min on a hot plate.

Characterization:

The X-ray diffraction (XRD) measurement was performed on Rigaku Miniflex with cobalt Kα radiation and the result was further converted into that of the copper target. Cross-sectional view of the device was obtained using a Field-Emission Scanning Electron Microscope (FE-SEM, JEOL 7100).

The current-voltage (I-V) plots were recorded using a solar simulator (AM 1.5, 100mW/cm^2, Oriel) equipped with a Keithley model 2420 digital source meter. The incident photon-to-current conversion efficiency (IPCE) measurement was performed on a Newport 1918-c power meter under the irradiation of a 300 W xenon light tower (Newport, 66902) with an Oriel CornerstoneT 260 ¼ m monochromator (Oriel, 74125) in DC mode.

Results and discussion

Fig 1(a) shows the scheme of the device structure, consisting of FTO/TiO_2 blocking layer (BL)/$CH_3NH_3PbI_{3-x}Cl_x$/P3HT/Au (denoted as device C1). The perovskite structure was confirmed by XRD measurement and the thickness of the perovskite film ranges from 0.8 µm to 2 µm (Fig S1.). Herein, we define the I-V scan from positive bias to 0 V as a reverse scan and the opposite direction as a forward scan. As shown in Fig. 1 (b and c), the I-V curves of the device are highly dependent on the initial positive bias. As the initial bias increases, all the cell parameters derived from the I-V curves are improved, showing a bias-dependent effect. In particular, increasing the initial positive bias from 1 V to 2.5 V leads to a significant enhancement of the short-circuit current density (J_{sc}) and open-circuit voltage (V_{oc}) by 31.1% and 13.4% respectively. It should be noted that a higher starting positive bias may possibly damage the device due to the possible degradation of organic components under high forward current and thus 2.5 V was chosen as the high bias limit.

This bias-dependent phenomenon is abnormal for solar cells because similar behaviour cannot be observed in either dye-sensitized solar cells or polycrystalline silicon solar cells (Fig. S2). Moreover, a "V"-shaped feature appears in the high positive bias range of the I-V curves, which disappears in the forward scan (Fig. S3). In order to explore the origin of the "V" shaped feature, current-time curves were performed both under illumination and dark, which show an exponential-like increase of the absolute current with time, indicating a slow process occurs under the high positive external bias (Fig. 1 (d)). Such a process takes more than 100 s to achieve a relative equilibrium value and contributes to the "V" shaped feature, since this feature disappears when performing the I-V scan immediately after 200 s poling at 1.5 V (Fig. S3 (b)). The exponential change of photocurrent to a constant bias has also been observed in a previous report and was related to a capacitive effect of the perovskite films.[11]

It has been demonstrated that the absolute current increased with time when a high external bias was applied to the device C1 and the device current increased rapidly during the first 50s when a constant external bias was applied (Fig. 1 (d)). Based on this observation, the "V-shape" feature of the I-V curves observed in the range from V_{oc} to the initial positive bias can be explained as follows. When performing the I-V scan forwardly, both the device current (absolute value) and the external bias increased simultaneously from V_{oc} to the initial positive bias, and thus the "V"-shaped feature in the I-V curve was absent (Fig S3 (a)). On the other hand, when the I-V scan was performed reversely, the device absolute current increased rapidly at the initial stage of the I-V scan while the bias reduced gradually, and thus a "V"-shaped feature appeared in the I-V curves. In brief, we can conclude that the electric response of the $CH_3NH_3PbI_{3-x}Cl_x$ film to the external bias is the origin of the "V"-shaped feature in the I-V curves.

Since the photocurrent density is highly dependent on the selected initial bias of the I-V scan, it is necessary to determine the actual photocurrent output by measuring the incident photon-to-electron conversion efficiency (IPCE) of the device C1 (Fig S4 (a)). It is rather surprising to find that the integrated photocurrent density (J_{sc}) from the IPCE is 6.2 mA/cm^2, significantly lower than that derived from the I-V measurement (Table 1). Therefore, we assumed that bias-dependent effect of the device might result in non-steady-state measurement of the I-V scans, especially at a high scan rate, leading to a significant J_{sc} deviation between the IPCE and I-V measurement. To examine this assumption, we further performed I-V scan based on the device C1 at an extremely slow scan rate (0.0005 V/s), so that the I-V data can represent more closely to the steady-state output of the device under measurement conditions. As shown in Fig S4 (b), the J_{sc} derived from this I-V curve is 7.07 mA/cm^2, much closer to that achieved by IPCE measurement. Hence, we can conclude that the bias-dependent effect can induce exaggerated photovoltaic parameters (i.e. J_{sc}, V_{oc}, FF and η) during the I-V measurement. To minimize the adverse bias-dependent effect on the I-V measurement, the initial bias should be close to the V_{oc} of the device under test and a slow I-V scan rate might be adopted during the I-V scan. The observations from these results also arise two key questions: (1) What is the origin of the bias-dependent effect? (2) Why do the V_{oc} and J_{sc} increase with the initial bias of the reverse scan?

In order to determine the origin of this phenomenon, a series of devices with planar structures of FTO/TiO_2 BL/$CH_3NH_3PbI_{3-x}Cl_x$/spiro-MeOTAD/Au, FTO/TiO_2 BL/$CH_3NH_3PbI_{3-x}Cl_x$/Au and FTO/$CH_3NH_3PbI_{3-x}Cl_x$/spiro-MeOTAD/Au were assembled. Interestingly, the bias-dependent effect was observed in all of these devices (Fig S5), suggesting that the perovskite itself might be the origin of the phenomenon. Since the organic-inorganic perovskite film can serve as a light-absorber and an electron/hole-transporting material simultaneously,[4] we also assembled a device with a structure of

FTO/$CH_3NH_3PbI_{3-x}Cl_x$/Au (denoted as device P1, Fig 2 (a)) in order to remove any possible effect from the P3HT and the TiO_2 BL. However, it is worth noting that such a capacitor-like structure might easily get short-circuited due to direct contact between the FTO and gold layer. To the best of our knowledge, there is no previous report on the I-V measurement based on such a device structure. However, characterizing the device P1 can provide direct evidence on the origin of the I-V hysteresis as well as the bias-dependent effect. In order to fabricate device with the structure of FTO/$CH_3NH_3PbI_{3-x}Cl_x$/Au, we tried to use the same spin-coating conditions as that of the device C1, whereas all the thus-assembled devices were failed due to short-circuit problem. To address the short-circuit problem, we modified the spin-coating conditions for fabricating the device P1 and ~ 3 µm-thick perovskite film was spun-coated on a pre-patterned FTO substrate (Fig 2 (b)), which finally showed normal I-V curves.

Firstly, we performed reverse and forward I-V scans in the range from 0 V to 1 V and found severe I-V hysteresis in this capacitor-like device (Fig 2 (c) and (d)). Since P3HT and TiO_2 BL layers were absent in this device, we can conclude that the I-V hysteresis should originate solely from the $CH_3NH_3PbI_{3-x}Cl_x$ film. To our knowledge, this is the first time to experimentally verify the direct relation between perovskite layer and the I-V hysteresis.

Different initial biases were applied to check whether the bias-dependent effect would exist in device P1. Indeed, the bias-dependent effect and a “V” shaped feature were observed in device P1 (Fig. 2 (e) and (f)), and thus we can conclude that the perovskite film is the origin of the bias-dependent effect as well as the “V”-shaped feature in the I-V curves. Moreover, the “V” shaped feature in the forward I-V scan curve disappears (Fig 2 (c)), which is in accordance with that of the device C1.

It is rather surprising to find that the V_{oc} and J_{sc} were improved by around 337.5% and 281.9% respectively by increasing the initial positive bias from 0.5 V to 2.5 V. Compared with the device C1, the bias dependent effect is much more significant in the device P1, which may be the result of a much thicker $CH_3NH_3PbI_{3-x}Cl_x$ film (~3 μm for P1, Fig. 2 (b)). The response of the perovskite film to the external bias was further confirmed by monitoring the current-time (I-t) relationship of the device P1 at a constant bias (Fig S6). We observed that the $CH_3NH_3PbI_{3-x}Cl_x$ film can respond to an external bias as low as 0.5 V. As such, it is clear that the effect of external bias on the $CH_3NH_3PbI_{3-x}Cl_x$ film should not be ignored in any I-V measurement of this system.

According to previous reports, it seems that the polarization of the perovskite film under external bias may be the possible reason for the bias-dependent phenomenon and that the "V"-shaped I-V curve in the high bias range might partially reflect the rearrangement of the perovskite films.[13, 17] . Frost *et al.* suggested that polarization of the perovskite film may occur due to the reorientation of the permanent dipoles (i.e. $CH_3NH_3^+$ and $[PbI_3]^-$) or dipole domains.[10, 13] During the polarization process, capacitive charge can be accumulated at the domain walls, which may contribute to the J_{sc} improvement observed in the bias-dependent effect.[7] Also, the existence of the ferroelectric domians in the organic-inorganic hybrid perovskite films has been confirmed by piezoforce microscopy.[18] Moreover, it has been demonstrated that the $CH_3NH_3PbI_{3-x}Cl_x$ film shows a Stark effect in perovskite/TiO_2 solar cells, which is due to a shift of transition energies of a molecule to an electric field, may cause a change of the V_{bi} (and hence V_{oc}) of the PSCs under different external bias.[23, 24] Such a Stark effect may explain the drastic V_{oc} improvement in the bias-dependent effect.

Moreover, it should be noted that the chemical and physical properties of the perovskite film are highly dependent on the film deposition method, which may affect the crystal

orientation and size, and in turn affect the rearrangement of the perovskite film in response to the external perturbations (i.e. bias and light illumination). [9, 11, 14, 25] Thus, this bias-dependent effect may be dependent on the perovskite film processing method as well. Moreover, ion migration (i.e. I^-, Cl^- and $CH_3NH_3^+$) within the perovskite film cannot be ruled out at this stage, which might play a role in I-V hysteresis phenomenon and the bias-dependent effect as well.[12] More detailed study is required to further confirm the proposed mechanism and theoretical modelling may provide more convincing explanation of the bias-dependent effect in the $CH_3NH_3PbI_{3-x}Cl_x$ based planar perovskite solar cells, all of which are now under investigation. Also, it is necessary to study whether ion migration might have any effect on the I-V hysteresis as well as the bias-dependent effect.

Conclusion

In summary, we have demonstrated in this study that $CH_3NH_3PbI_{3-x}Cl_x$ based planar perovskite solar cells exhibit a significant bias-dependent effect in the current-voltage measurement. All of the cell parameters derived from the I-V measurement can be improved substantially by performing the reverse scan from a high initial positive bias. Moreover, we provide direct evidence to confirm that both the bias-dependent effect and I-V hysteresis phenomenon are resulted from the $CH_3NH_3PbI_{3-x}Cl_x$ layer itself, which has not been reported previously. Polarization of the perovskite film due to the electric-field response of the polar $CH_3NH_3PbI_{3-x}Cl_x$ was proposed to play a role in such a bias-dependent effect. These new findings and understanding of the external bias-dependent effect in organic-inorganic perovskite solar cells provide more insight into the intrinsic behaviour of the $CH_3NH_3PbI_{3-x}Cl_x$ films, such as the well-known I-V hysteresis, giant dielectric constant and charge accumulation in this new family of solar cells. More importantly, such a significant influence

of the bias on the device measurement suggests that the initial scan bias conditions and I-V scan rate should be selected carefully when performing the I-V measurement. Further characterization of the capacitive effect, which may be an important factor in properties of perovskite solar cells, is required. Furthermore, the significant capacitance effect in the $CH_3NH_3PbI_{3-x}Cl_x$ film as well as its slow dynamic response to the bias may find application in other electronic devices.

Appendix A: Supplementary material

Acknowledgement

Financial support from Cooperative Research Centre for Polymer (CRC-P) programs and ARC DPs and FT programs is acknowledged. This work was performed in part at the Queensland node of the Australian National Fabrication Facility and the Australian Microscopy & Microanalysis Research Facility at the Centre for Microscopy and Microanalysis, the University of Queensland. M.Q. Lyu acknowledges the support from IPRS Scholarship.

References

[1] J. Burschka, N. Pellet, S.-J. Moon, R. Humphry-Baker, P. Gao, M.K. Nazeeruddin, M. Grätzel, Nature, 499 (2013) 316-319.

[2] N.J. Jeon, J.H. Noh, Y.C. Kim, W.S. Yang, S. Ryu, S.I. Seok, Nat Mater., (2014) DOI: 10.1038/nmat4014

[3] M. Liu, M.B. Johnston, H.J. Snaith, Nature, 501 (2013) 395-398.

[4] S.D. Stranks, G.E. Eperon, G. Grancini, C. Menelaou, M.J. Alcocer, T. Leijtens, L.M. Herz, A. Petrozza, H.J. Snaith, Science, 342 (2013) 341-344.

[5] E.J. Juárez-Pérez, R.S. Sánchez, L. Badia, G. Garcia-Belmonte, Y.S. Kang, I. Mora-Sero, J. Bisquert, J. Phys. Chem. Lett., 5 (2014) 2390-2394.
[6] H.S. Kim, I. Mora-Sero, V. Gonzalez-Pedro, F. Fabregat-Santiago, E.J. Juarez-Perez, N.G. Park, J. Bisquert, Nat Commun, 4 (2013) 2242.
[7] R.S. Sanchez, V. Gonzalez-Pedro, J.-W. Lee, N.-G. Park, Y.S. Kang, I. Mora-Sero, J. Bisquert, J. Phys. Chem. Lett., 5 (2014) 2357-2363.
[8] H.J. Snaith, A. Abate, J.M. Ball, G.E. Eperon, T. Leijtens, N.K. Noel, S.D. Stranks, J.T.-W. Wang, K. Wojciechowski, W. Zhang, J. Phys. Chem. Lett., 5 (2014) 1511-1515.
[9] R. Gottesman, E. Haltzi, L. Gouda, S. Tirosh, Y. Bouhadana, A. Zaban, E. Mosconi, F. De Angelis, J. Phys. Chem. Lett., (2014) 2662-2669.
[10] J.M. Frost, K.T. Butler, A. Walsh, Apl Materials, 2 (2014) 081506.
[11] H.S. Kim, N.-G. Park, J. Phys. Chem. Lett., DOI: 10.1021/jz501392m (2014).
[12] E.L. Unger, E.T. Hoke, C.D. Bailie, W.H. Nguyen, A.R. Bowring, T. Heumuller, M.G. Christoforo, M.D. McGehee, Energy Environ Sci, (2014) DOI: 10.1039/C4EE02465F
[13] J.M. Frost, K.T. Butler, F. Brivio, C.H. Hendon, M. van Schilfgaarde, A. Walsh, Nano Lett, 14 (2014) 2584-2590.
[14] J. Wei, Y. Zhao, H. Li, G. Li, J. Pan, D. Xu, Q. Zhao, D. Yu, J Phys Chem Lett, (2014) 3937-3945.
[15] B. Chen, X. Zheng, M. Yang, Y. Zhou, S. Kundu, J. Shi, K. Zhu, S. Priya, Nano Energy, DOI:10.1016/j.nanoen.2015.03.037 (2015).
[16] H.-W. Chen, N. Sakai, M. Ikegami, T. Miyasaka, J Phys Chem Lett, 6 (2014) 164–169.
[17] F. Brivio, A.B. Walker, A. Walsh, APL Materials, 1 (2013) 042111.
[18] Y. Kutes, L. Ye, Y. Zhou, S. Pang, B.D. Huey, N.P. Padture, J Phys Chem Lett, 5 (2014) 3335-3339.
[19] S. Colella, E. Mosconi, G. Pellegrino, A. Alberti, V.L.P. Guerra, S. Masi, A. Listorti, A. Rizzo, G.G. Condorelli, F. De Angelis, G. Gigli, J Phys Chem Lett, (2014) 3532-3538.
Y. Kinoshita, R. Takenaka, H. Murata, Appl. Phys. Lett., 92 (2008) 243309.
[20] J.A. McLeod, Z. Wu, P. Shen, B. Sun, L. Liu, J Phys Chem Lett, 5 (2014) 2863-2867.
[21] Y. Kinoshita, R. Takenaka, H. Murata, Appl Phys Lett, 92 (2008) 243309.
[22] V. Roiati, E. Mosconi, A. Listorti, S. Colella, G. Gigli, F. De Angelis, Nano Lett, 14 (2014) 2168-2174.
[23] E. Siebert-Henze, V. Lyssenko, J. Fischer, M. Tietze, R. Brueckner, T. Menke, K. Leo, M. Riede, Organic Electronics, 15 (2014) 563-568.

[24] E. Siebert-Henze, V.G. Lyssenko, J. Fischer, M. Tietze, R. Brueckner, M. Schwarze, K. Vandewal, D. Ray, M. Riede, K. Leo, AIP Advances, 4 (2014) 047134.
[25] C.C. Stoumpos, C.D. Malliakas, M.G. Kanatzidis, Inorg Chem, 52 (2013) 9019-9038.

Table 1 Cell parameters derived from the I-V curves of C1 using different initial bias. The aperture area is 0.07 cm^2. (Note: J_{sc}, V_{oc}, FF and η% correspond to photocurrent density, open-circuit voltage, fill factor and efficiency, respectively)

Initial bias	**J_{sc}/mA/cm^2**	**V_{oc}/V**	**FF**	**η %**
1 V	17.40	0.67	0.45	5.25
1.5 V	19.38	0.72	0.53	7.40
2 V	20.23	0.76	0.58	8.86
2.5 V	20.51	0.76	0.59	9.17

Table 2 Cell parameters derived from the I-V curves of P1 using different initial bias. The aperture area is 0.07 cm^2.

Initial bias	**J_{sc}/mA/cm^2**	**V_{oc}/V**	**FF**	**η%**
0.5 V	6.37	0.16	0.27	0.27
1 V	12.80	0.32	0.33	1.34
1.5 V	20.48	0.60	0.42	5.17
2 V	23.36	0.68	0.50	7.98
2.5 V	24.33	0.70	0.48	8.19

Figure Captions:

Fig. 1 (a) Schematic diagram of the perovskite solar cell structure (device C1); (b) I-V curves of the device C1 reversely scanned from different initial biases under AM 1.5, 100 mW/cm^2 solar irradiation and the scan rate is 0.1 V/s; (c) The enlarged view of the I-V curves in the bias range between 0 V to 1 V; (d) Current-time curves of device C1 at a constant external bias of 1.5 V under illumination and dark.

Fig. 2 (a) Schematic diagram of the device P1 with a structure of FTO/ $CH_3NH_3PbI_{3-x}Cl_x$ /Au; (b) Cross-sectional SEM image of the device P1; I-V curves of the device P1, which was performed reversely (black curve) and forwardly (red curve) under AM 1.5, 100 mW/cm^2 solar irradiation with a scan rate of 0.1 V/s: (c) full scale I-V curves from 0 V to 1 V; (d) Enlarged I-V curves of (c) between 0 V and 0.4 V. (e) I-V curves of the device P1 reversely scanned from different initial biases under AM 1.5, 100 mW/cm^2 solar irradiation and the scan rate is 0.1 V/s; (f) The enlarged view of (e) in the bias range between 0 V to 0.8 V.

Fig. 1

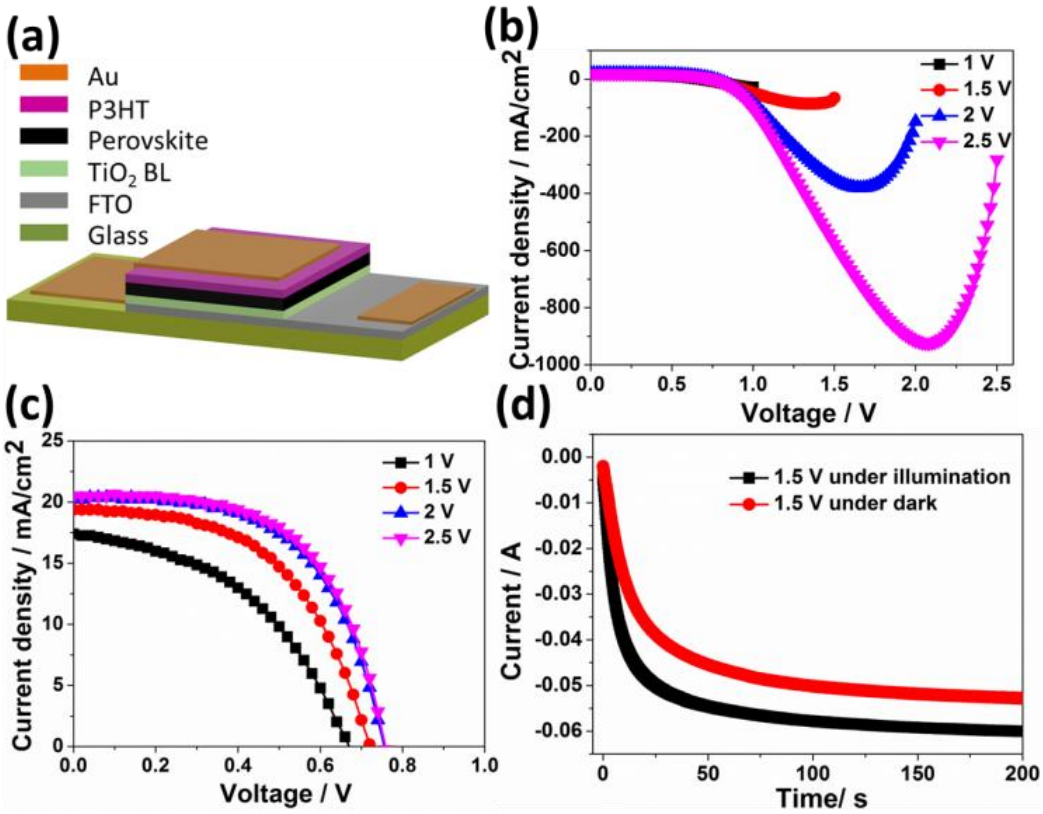
(a)
Au
P3HT
Perovskite
TiO2 BL
FTO
Glass
(b)
Current density / mA/cm2
Voltage / V
1 V
1.5 V
2 V
2.5 V
(c)
Current density / mA/cm2
Voltage / V
1 V
1.5 V
2 V
2.5 V
(d)
Current / A
Time/ s
1.5 V under illumination
1.5 V under dark

Fig. 2

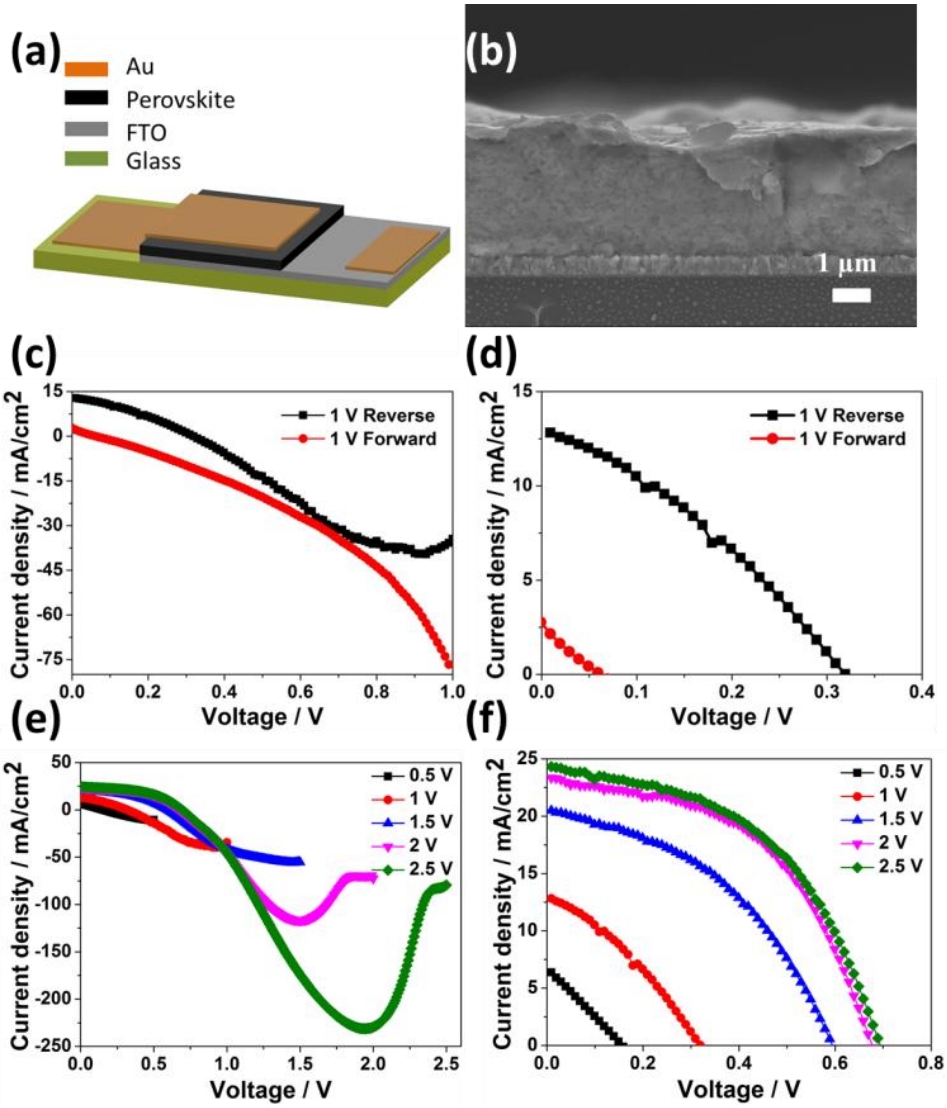
(a)
Au
Perovskite
FTO
Glass
(b)
1 μm
(c)
1 V Reverse
1 V Forward
Current density / mA/cm2
Voltage / V
(d)
1 V Reverse
1 V Forward
Current density / mA/cm2
Voltage / V
(e)
0.5 V
1 V
1.5 V
2 V
2.5 V
Current density / mA/cm2
Voltage / V
(f)
0.5 V
1 V
1.5 V
2 V
2.5 V
Current density / mA/cm2
Voltage / V

Graphic Abstract

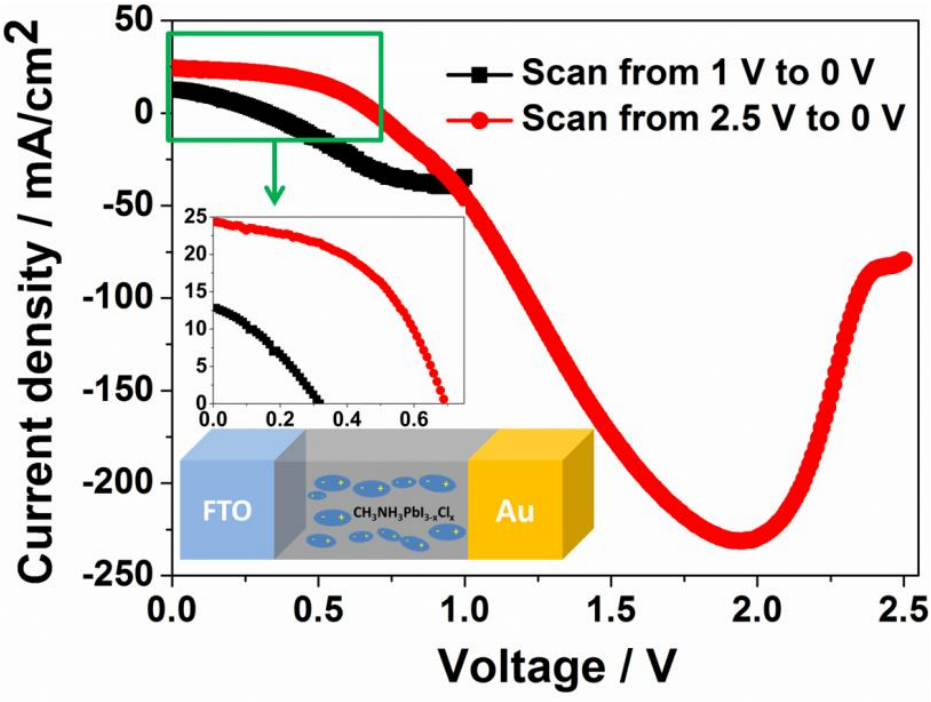

Highlights

A unique bias-dependent phenomenon in $CH_3NH_3PbI_{3-x}Cl_x$ based planar perovskite solar cells is reported

Photovoltaic parameters derived from the current-voltage measurement are highly dependent on the initial positive bias

Direct experimental evidence has been provided to verify the origin of current-voltage hysteresis and bias-dependent effect